

# Topological phases due to the coexistence of superconductivity and spin-density wave: Application to high $T_c$ superconductors in the underdoped regime

Amit Gupta\* and Debanand Sa†  
Department of Physics,  
Banaras Hindu University, Varanasi-221 005

(Dated: January 6, 2014)

We consider the coexistence of superconductivity(SC) and spin-density wave(SDW). The SC is presumed to be of  $d_{x^2-y^2} + id_{xy}(d_1 + id_2)$  type whereas the SDW order parameter is of  $BCS/d_{xy}$  symmetry. The Hamiltonian having such a structure is shown to have topological coexistence phases in addition to the conventional one. It is shown that the amplitudes of both the order parameters determine the nature of topological phases. A phase diagram characterizing different topological phases with their Chern numbers are obtained. The experimental realization of such topological phases with reference to high temperature superconductors in the extreme underdoped regime are discussed.

**PACS numbers:** 74.20.Fg, 74.90.+n, 71.10.Fd, 73.43.-f

Various quantum states of matter are described by the principle of spontaneous symmetry breaking [1]. For example, a crystalline solid breaks translational symmetry whereas magnetism breaks rotational symmetry and a superconductor breaks the more subtle gauge symmetry. This class of symmetry breaking phenomena are described by a unique order parameter which yields a non-vanishing expectation value only in the ordered state. This phenomena is described by an effective field theory, known as Landau-Ginzburg theory. However, the discovery of quantum Hall effect (QHE) [2] in early 1980's gave rise to a new states of matter which cannot be understood by the above mentioned Landau's symmetry breaking paradigm. In the quantum Hall (QH) state, the bulk of the two-dimensional (2D) sample is insulating and the electric current is carried only along the edge of the sample. The flow of this unidirectional current avoids dissipation and gives rise to quantized Hall conductance. The QH state provided the first example of a quantum state which is topologically distinct from all states of matter known before. The precise quantization of the Hall conductance is explained by the fact that it is topological invariant, independent of the material parameters [4, 21] and cannot change unless the system passes through a quantum phase transition. The QH states belong to a class which explicitly breaks time-reversal (TR) symmetry due to the presence of magnetic field. In last few years, a new class of topological phase has been theoretically predicted in two dimensional systems in presence of time-reversal symmetry and experimentally observed in HgTe quantum wells (QW's). In achieving topological insulator, the spin-orbit coupling (SOC) plays an essential role [5–8]. This quantum Hall phase is distinguished from a band insulator by a single  $Z_2$  invariant. This phase exhibits gapless spin-filtered edge-states, which al-

low for dissipationless transport of charge and spin at zero temperature and are protected from weak disorder and interactions due to time-reversal symmetry. In 2007, this effects is also observed in three-dimensional (3D) systems whose surface states are spin-polarized 2D metals and are characterized by four  $Z_2$  invariants. The topological concept is applied to both insulators and superconductors which have full energy gap. It is also worth mentioning that one gapped state can not be deformed into another gapped state in a different topological class unless a quantum phase transition occurs when the system become gapless.

In what follows, we consider the coexistence of SC and SDW. The SC is considered to be of  $d_1 + id_2$  type whereas the SDW order parameter is of  $BCS/d_{xy}$  symmetry. Such a Hamiltonian is shown to yield topological coexistence phases in addition to the conventional one. It is shown that the the amplitudes of both the order parameters determine the topological phases. The Chern number and hence the nature of the topological phases are determined. A phase diagram characterizing different topological phases are obtained. The experimental realization of such topological phases are discussed.

High magnetic field measurements in high temperature [9] SC have not only shown the persistence of SC but also a plateau region. This is thought to be due to development of a small  $d_{xy}$  component of the SC order parameter to the principal component  $d_{x^2-y^2}$ . Some other experiments in presence of magnetic field [10–13] indicated strong evidence for the onset of translational symmetry breaking density wave order. Further, recent angle resolved photo-emission spectroscopy (ARPES) experiments done on the deeply underdoped cuprate samples which are at the border between the antiferromagnetic (AF) and SC phase have revealed a full particle-hole symmetry (PHS) gap for  $\text{Bi}_2\text{Sr}_2\text{CaCu}_2\text{O}_{8+\delta}$  (Bi2212) [14, 15],  $\text{La}_{2-x}\text{Sr}_x\text{CuO}_4$  (LSCO)[16, 17],  $\text{Bi}_2\text{Sr}_{2-x}\text{La}_x\text{CuO}_{6+\delta}$  (Bi2201)[18] and  $\text{Ca}_{2-x}\text{Na}_x\text{CuO}_2\text{Cl}_2$  (NaCCOC)[19]. Such a gap along

\* sunnyamit31@gmail.com

† debanandsa@rediffmail.com

the nodal direction has been observed in systems whose magnetic and transport properties range from AF insulator to SC. This data is in excellent agreement with the mixed  $d_1 + id_2$  SC along the entire Fermi surface. Thus, it is worth addressing the physics of the coexistence phase of SC and SDW with the above mentioned symmetries of the order parameters. The mean-field treatment of such a coexistence of  $d_1 + id_2$  SC and  $d_{xy}$  SDW in a 2D square lattice is described by the Hamiltonian  $\mathcal{H} = \mathcal{H}_{\text{kin}} + \mathcal{H}_{\text{sc}} + \mathcal{H}_{\text{SDW}}$ ,

$$\begin{aligned} \mathcal{H}_{\text{kin}} &= \sum_{k,\sigma} \epsilon_k c_{k,\sigma}^\dagger c_{k,\sigma} \\ \mathcal{H}_{\text{sc}} &= \sum_k (\Delta_k c_{k,\uparrow}^\dagger c_{-k,\downarrow}^\dagger \\ &\quad + \Delta_{k+Q} c_{k+Q,\uparrow}^\dagger c_{-k-Q,\downarrow}^\dagger + H.C.) \\ \mathcal{H}_{\text{SDW}} &= \sum_{k,\sigma} (\sigma M_k c_{k,\sigma}^\dagger c_{k+Q,\sigma} + H.C.), \end{aligned} \quad (1)$$

where  $c_{k\sigma}^\dagger$  ( $c_{k\sigma}$ ) denotes creation (annihilation) operator of the electron with spin  $\sigma = (\uparrow, \downarrow)$  at  $\mathbf{k} = (k_x, k_y)$  and  $\epsilon_k = -2t(\cos k_x a + \cos k_y a) - \mu$ ,  $\Delta_k = \Delta_{1,k} + i\Delta_{2,k} = \Delta_1 \left( \frac{\cos k_x a - \cos k_y a}{2} \right) + i\Delta_2 (\sin k_x a \sin k_y a)$  is  $d_1 + id_2$ -wave SC order parameter,  $M_k = \lambda_0 \sin k_x a \sin k_y a$  is the SDW order parameter and  $\mu$  is the chemical potential. We express momenta in units of  $\frac{\pi}{a}$ , with 'a' the lattice parameter of the underlying square lattice. The self-consistent equations for  $\Delta_k$  and  $M_k$  can be written as,  $\Delta_k = \sum_{k'} g_{kk'} \langle c_{-k',\downarrow} c_{k',\uparrow} \rangle$  and  $M_k = \sum_{k',\sigma} \frac{J_{kk'}}{2} \sigma \langle c_{k',\sigma}^\dagger c_{k+Q,\sigma} \rangle$ , where  $g_{k,k'}$  and  $J_{k,k'}$  respectively are the microscopic interactions inducing SC and SDW. In the momentum space, the Hamiltonian can be recasted into  $\mathcal{H} = \sum_k \psi_k^\dagger \mathcal{H}(k) \psi_k$  where the four-component spinor  $\psi_k$  is,  $\psi_k^\dagger = (c_{k\uparrow}^\dagger, c_{-k\downarrow}, c_{k+Q\uparrow}^\dagger, c_{-k-Q\downarrow})$  with  $\mathcal{H}(k)$  as,

$$\mathcal{H}(k) = \begin{pmatrix} \epsilon_k - \mu & \Delta_k & M_k & 0 \\ \Delta_k^* & -\epsilon_k + \mu & 0 & M_k \\ M_k & 0 & \epsilon_{k+Q} - \mu & \Delta_{k+Q} \\ 0 & M_k & \Delta_{k+Q}^* & -\epsilon_{k+Q} + \mu \end{pmatrix}. \quad (2)$$

Employing the nesting property i.e.  $\epsilon_{k+Q} = -\epsilon_k$ , where  $Q = (\pi, \pi)$  is the nesting wave vector. Also,  $\Delta_{k+Q} = \Delta_{1,k+Q} + i\Delta_{2,k+Q} = -\Delta_1 \left( \frac{\cos k_x - \cos k_y}{2} \right) + i\Delta_2 \sin k_x \sin k_y = -\Delta_{1,k} + i\Delta_{2,k} = -\Delta_k^*$  and  $M_{k+Q} = \lambda_0 \sin k_x \sin k_y = M_k$ . Thus, the above Hamiltonian matrix reduces to,

$$\mathcal{H}(k) = \begin{pmatrix} \epsilon_k - \mu & \Delta_k & M_k & 0 \\ \Delta_k^* & -\epsilon_k + \mu & 0 & M_k \\ M_k & 0 & -\epsilon_k - \mu & -\Delta_k^* \\ 0 & M_k & -\Delta_k & \epsilon_k + \mu \end{pmatrix}. \quad (3)$$

We will study the phase diagram of the above Hamiltonian for  $\mu = 0$ . The bulk quasiparticle spectrum is,  $E_{\sigma,\pm}(k) = \sigma \sqrt{\epsilon_k^2 + \Delta_{1,k}^2 + (\Delta_{2,k} \pm M_k)^2}$  which shows fully gapped structure as shown in Fig.1. Considering

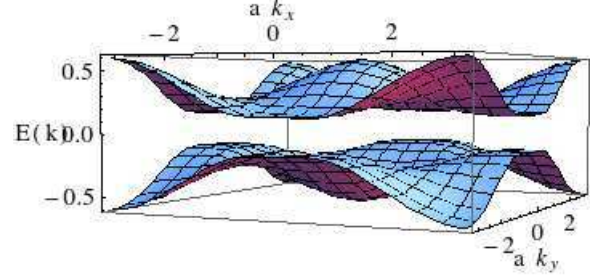


FIG. 1. Energy spectra  $E_{\sigma,+}(k)$ , corresponding to coexistence of SC order parameter  $d_{x^2-y^2} + id_{xy}$  and that of the SDW order parameter (BCS-type) showing fully gapped structure. For illustration, here, we have chosen  $M_0 = .11$  eV,  $\Delta_1 = \Delta_2 = t$  ( $t = 0.15$  eV. The chemical potential  $\mu$  is taken to be zero.

the case where  $\langle M_k \rangle = 0$  but retaining the density-wave fluctuations, the above Hamiltonian can be written as,

$$\mathcal{H}(k) = \begin{pmatrix} h(k) & 0 \\ 0 & -h^*(-k) \end{pmatrix}, \quad (4)$$

where  $h(k) = \epsilon_k \sigma_z + \Delta_{1,k} \sigma_x - \Delta_{2,k} \sigma_y$  and  $h^*(-k) = \epsilon_k \sigma_z + \Delta_{1,k} \sigma_x + \Delta_{2,k} \sigma_y$  and  $\sigma_x, \sigma_y$  and  $\sigma_z$  are respectively the Pauli matrices. The above equation is the Hamiltonian of a standard  $d_1 + id_2$  superconductor which behaves as a quantum spin Hall fluid (QSHF) [20–22] giving rise to spin Hall conductance quantization. This Hamiltonian has particle-hole symmetry (PHS) and a class C with  $SU(2)$  symmetry classification of Altland and Zirnbauer [23, 24]. However, the presence of  $M_k$  breaks particle-hole symmetry. The topological phases can be characterized by the *Chern number*. For a specific model Hamiltonian  $h(k) = \sum_{\alpha} d_{\alpha}(k) \sigma_{\alpha}$ , with  $\sigma_{\alpha}$ , the Pauli matrices and  $d_{\alpha}(k) = [d_1(k), d_2(k), d_3(k)]$ , the Chern number can be calculated from the expression

$$\mathcal{N} = \frac{1}{4\pi} \int d^2k \, \hat{d}(\hat{k}) \cdot \left( \frac{\partial \hat{d}(k)}{\partial k_x} \times \frac{\partial \hat{d}(k)}{\partial k_y} \right), \quad (5)$$

where the unit vector  $\hat{d}(k) = \mathbf{d}(k) / \sqrt{\sum d^2(k)}$ . Following Volovik [20] and Senthil [22] the Chern number of the above Hamiltonian is calculated as  $\mathcal{N} = 2 \text{sgn}(\Delta_1 \Delta_2)$  in units of  $(\hbar/8\pi)$ . This is true for each block of the Hamiltonian (4). This results remains unchanged even if one includes the nesting fluctuations in the  $d_1 + id_2$  superconductor. It is well known from the theory of Quantum Hall effect that the quantization of bulk charge/spin Hall conductance implies the existence of boundary states carrying charge/spin. In the present case the boundary states carry spin. This is due to the fact that each block in eqn.(4) can be linearized near the nodal points of the

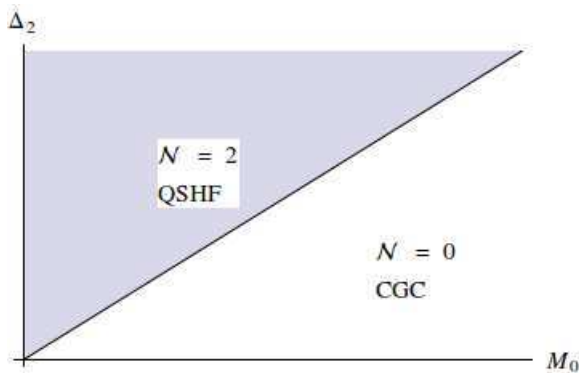


FIG. 2. Schematic phase diagram of the coexistence phase of SC  $d_1 + id_2$  order and BCS-type SDW order for  $\mu = 0$  in the case where  $k = (\pm\pi/2, \pm\pi/2)$ . The  $x$  axis labels the magnitude of SDW order parameter  $M_0$  and the  $y$  axis labels the magnitude of SC order parameter  $\Delta_2$ . Integer  $\mathcal{N}$  labels the Chern number of the coexistence of SC and SDW.

square lattice Brillouin Zone. The  $d_{x^2-y^2}$  SC part of the Hamiltonian makes it Dirac Hamiltonian and  $d_{xy}$  part adds a mass term to it. From such a structure an effective edge Hamiltonian is worked out. Since the edge density operator is proportional to the  $z$ -component of spin, it gives rise to non-zero spin Hall conductance.

In presence of finite  $M_k$ , the above Hamiltonian matrix can be written as,

$$\mathcal{H}(k) = \begin{pmatrix} h(k) & M_k \sigma_0 \\ M_k \sigma_0 & -h^*(-k) \end{pmatrix}. \quad (6)$$

The above Hamiltonian (Eqn.(6)) can be block diagonalized through a unitary transformation

$$\mathcal{H}^D(k) = D\mathcal{H}(k)D^\dagger, \quad D = \frac{1}{\sqrt{2}} \begin{pmatrix} 1 & -\sigma_y \\ \sigma_y & 1 \end{pmatrix}, \quad (7)$$

with

$$\mathcal{H}^D(k) = \begin{pmatrix} h_{UB}(k) & 0 \\ 0 & -h_{LB}(-k) \end{pmatrix}, \quad (8)$$

where,  $h_{UB}(k) = \epsilon_k \sigma_z + \Delta_{1,k} \sigma_x - (\Delta_{2,k} + M_k) \sigma_y$  and  $h_{LB}(k) = \epsilon_k \sigma_z + \Delta_{1,k} \sigma_x + (\Delta_{2,k} - M_k) \sigma_y$ . It is obvious from the Hamiltonian that the presence of the order parameter  $M_k$  breaks particle-hole symmetry.

In order to study the phase diagram of this Hamiltonian in the  $(\Delta_2, M_0)$  plane, one needs to determine the phase boundaries corresponding to gapless regions since the topological invariants can not change without closing the bulk gap. For the present model, the critical lines are determined by the equation  $|\Delta_2 \pm M_0| = 0$  in the case with  $\mathbf{k} = (\pm\pi/2, \pm\pi/2)$  which leads to a phase diagram shown in Fig. 2. If one considers the SDW order parameter to be of BCS type (constant  $M_0$ ), then the line  $M_0 = \Delta_2$  yields a phase boundary between the topological phase (QSHF for  $M_0 < \Delta_2$ ) and the conventional gapped coexistent (CGC) SDW and SC phase.

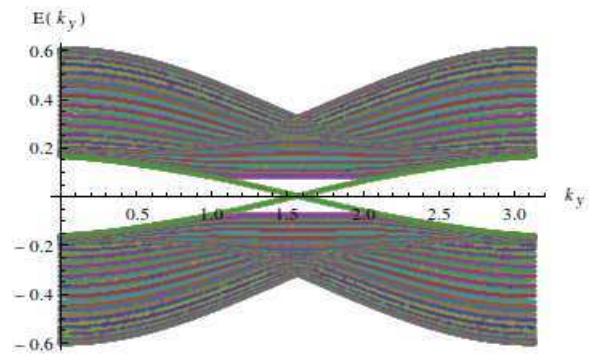


FIG. 3. Edge state spectrum of the coexistence phase of SC  $d_1 + id_2$  order and BCS-type SDW order on a cylinder. Parameters are chosen as,  $t = 0.15$  eV,  $M_0 = .075$  eV and  $\Delta_1 = \Delta_2 = t$  for a lattice of  $N_x = 80$  sites.

The Chern number in the case  $M_0 < \Delta_2$  is  $\mathcal{N} = 2$  whereas it vanishes for  $M_0 > \Delta_2$  till it touches  $\Delta_2 = 0$  line. Keeping  $M_0$  fixed and varying  $\Delta_2$  from zero to higher values, one passes from CGC(non-topological) to QSHF(topological) phase through a quantum phase transition ( $|\Delta_2 \pm M_0|$ ) line. This is due to the fact that on increasing  $\Delta_2$ , band inversion occurs and one enters into the topological phase from an ordinary phase. In case of  $M_k$  having  $d_{xy}$  symmetry,  $M_0 > \Delta_2$  phase also becomes topological which is distinct from  $M_0 < \Delta_2$  case. The Chern number in this case can be inferred from the  $\Delta_2 = 0$  and  $M_0 \neq 0$  line.

In order to see the edge state evolution, we have studied the edge states numerically on a cylinder geometry with periodic boundary conditions in the  $y$ -direction and open boundary conditions in the  $x$ -direction as shown in Fig 3. The BdG Hamiltonian (Eqn.(3)) has been diagonalized on  $N_x = 80$  sites and the energy dispersion  $E_k$  versus  $k_y$  with edge states has been obtained. As already mentioned, two chiral edge states characterize the topological QSHF phase.

An intuitive way to understand the topological QSHF state for  $M_0 = 0$  case is the evolution of edge states. Such a phase is described by an effective one-dimensional Hamiltonian  $H_{edge} = \sum_k v k \eta_k^\dagger \eta_k$ , where  $\eta_k$ 's are the complex fermion operators. These are a pair of chiral fermions from each of the four nodal points in the Brillouin Zone which give rise to Chern number  $\mathcal{N} = 2$ . Along the  $\Delta \neq 0$  and  $M_0 = 0$  line, the  $d_1 + id_2$  edge states evolve independently. The edge states with  $k = (\pm\pi/2, \pm\pi/2)$  has width  $\xi \sim |\Delta_2|^{-1}$ . But in the case of finite  $M_0$  ( $M_0 < \Delta_2$ ), the widths are  $\xi_1 \sim |\Delta_2 - M_0|^{-1}$  and  $\xi_2 \sim |\Delta_2 + M_0|^{-1}$ . As  $M_0$  increases the localization length  $\xi$  of the edge modes diverge and gradually they merge into bulk states. At the critical line  $|\Delta_2 \pm M_0| = 0$ , these edge states completely merge into the bulk states and the system become gapless. For  $\Delta_2 < M_0$ , again a gap opens up and the system becomes the CGC phase. The present study analyzes the possibility of having topological phases in the coexistence phase of SC-SDW, how-

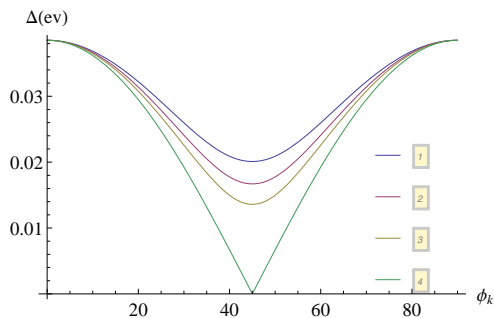


FIG. 4. Calculated energy gap  $\Delta_k = |\Delta_{1,k} + i(\Delta_{2,k} \pm M_0)|$  as a function of Fermi surface angle  $\phi_k$  where  $\Delta_1=38.52$  meV and from top to bottom  $\Delta_2 = 20, 16.6, 13.6$  and  $0.0$  meV respectively consistent with [17].

ever on the contrary, there exists literature either in chiral SC from quantum Hall systems[25] or in topological insulators in a perpendicular magnetic field[26] as well as topological insulating nanowires proximity to SC in longitudinal magnetic field[27].

It has already been known from neutron scattering measurements[28] that there are strong indications of the presence of static/fluctuating SDW order below optimal doping at low temperature. The profound departure from the  $d_{x^2-y^2}$  SC along the nodal direction and the entire gapped Fermi surface in the highly underdoped LSCO ( $x=0.08$ ) suggest that the effective gap of the present kind, i.e.,  $\Delta(k) = |\Delta_{1,k} + i(\Delta_{2,k} \pm M_0)|$  might be at work. Considering  $\Delta_{1,k} = \Delta_1 \cos 2\phi_k$ ,  $\Delta_{2,k} = (\frac{\Delta_2}{2}) \sin 2\phi_k$  one can compute the effective gap  $\Delta(\phi_k)$  as a function of  $\phi_k$ . The observed gap [17] has a maximum value at the zone boundary ( $\phi_k = 0$ ) and decreases monotonically along the Fermi surface to a minimum value at the zone diagonal ( $\phi_k = \pi/4$ ). Below  $T_c$  (20 K), a finite gap of amplitude  $\sim 20$  meV along the zone diagonal has been observed. As temperature

increases, the diagonal gap monotonically decreases and disappears at 88 K. At higher temperature, Fermi arc appears and the arc length increases with temperature. Following [17], we take  $\Delta_1=38.52$  meV to fit the data which yields  $\Delta_2=20, 16.6, 13.5, 0$  meV (from top to bottom in Fig.4) for  $M_0/\Delta_2 = 10^{-4}$ . This is in excellent agreement with the experiment data along the entire Fermi surface. Recently, there is an attempt [17] to explain the data with a pure  $d_1 + id_2$  SC but the question of whether the SDW ordering is present remains open. However, the present study takes into account of SDW ordering along with  $d_1 + id_2$  SC which explains the data very well for extremely small value of SDW order parameter  $M_0$  mentioned above. Further, it unfolds the topological aspects which might be crucial for further understanding of high  $T_c$  SC. Similar approach has been initiated recently for  $(p + ip)_{\uparrow\downarrow}$  SC in presence of SDW ordering [29].

In conclusion, we summarize the contents of the paper. Motivated by high magnetic field, neutron scattering and ARPES measurements, we considered a coexistence of  $d + id$  SC and BCS like SDW. It has been shown that for SC order parameter ( $\Delta_2$ )  $>$  SDW order parameter ( $M_0$ ) the system becomes topological whereas for  $\Delta_2 < M_0$  it is conventional coexistence phase. In terms of the amplitude of both the order parameters  $\Delta_2$  and  $M_0$  a phase diagram characterizing both the phases are obtained. The effective gap is computed for the entire Fermi surface which is in excellent agreement with the observed ARPES data for extremely small value of the SDW order parameter. The present analysis might help to understand the issue of whether the deep underdoped regime in high  $T_c$  is characterized by SDW ordering.

## ACKNOWLEDGEMENTS

Financial supports from CSIR, India are gratefully acknowledged.

- 
- [1] P. W. Anderson, *Basic Notions of Condensed Matter Physics* (Westview Press, Boulder, CO) (1997).  
[2] K. Von Klitzing, G. Dorda and M. Pepper, Phys. Rev. Lett. **45**, 494 (1980).  
[3] R. B. Laughlin, Phys. Rev. B **23**, 5632 (1981).  
[4] D. J. Thouless, M. Kohmoto, M. P. Nightingale, and M. den Nijs, Phys. Rev. Lett. **49**, 405 (1982).  
[5] M. König, H. Buhmann, L. W. Molenkamp, T. L. Hughes, C. X. Liu, X. L. Xi and S. C. Zhang, J. Phys. Soc. Jpn. **77**, 031007 (2008).  
[6] J. E. Moore, Nature (London) **464**, 194 (2010).  
[7] M. Z. Hasan and C. L. Kane, Rev. Mod. Phys. **82**, 3045 (2010).  
[8] X. L. Qi and S. C. Zhang, Phys. Today **63**, 33 (2010).  
[9] K. Krishana, N. P. Ong, Q. Li, G. D. Gu and N. Koshizuka, Science **277**, 83 (1997).  
[10] B. Lake, G. Aeppli, K. N. Klausen, D. F. McMorrow, K. Lefmann, N. E. Hussey, N. Mangkerntong, M. Nohara, H. Takagi, T. E. Mason, and A. Schröder, Science **291**, 1759 (2001).  
[11] B. Khaykovich, S. Wakimoto, R. J. Birgeneau, M. A. Kastner, Y. S. Lee, P. Smeibidl, P. Vorderwisch and K. Yamada, Phys. Rev. B. **47**, 220508 (2005).  
[12] J. Chang, N. B. Christensen, C. Niedermayer, K. Lefmann, H. M. Ronnow, D. F. McMorrow, A. Schneidewind, P. Link, A. Hiess, M. Boehm, R. Mottl, S. Pailhes, N. Momono, M. Oda, M. Ido, and J. Mesot, Phys. Rev. Lett. **102**, 177006 (2009).  
[13] D. Haug, V. Hinkov, A. Suchanek, D. S. Inosov, N. B. Christensen, C. Niedermayer, P. Bourges, Y. Sidis, J. T. Park, A. Ivanov, C. T. Lin, J. Mesot, and B. Keimer, Phys. Rev. Lett. **103**, 017001 (2009).  
[14] K. Tanaka, W. S. Lee, D. H. Lu, A. Fujimori, T. Fujii, Risdiana, I. Terasaki, D. J. Scalapino, T. P. Devereaux,

- Z. Hussain, *Science* **314**, 1910 (2006).
- [15] I. M. Vishik, M. Hashimoto, R. -H. He, W. -S. Lee, F. Schmitt, D. Lu, R. G. Moore, C. Zhang, W. Meevasana, T. Sasagawa, *Proceedings of the National Academy of Sciences* **109**, 18332 (2012).
- [16] A. Ino, C. Kim, M. Nakamura, T. Yoshida, T. Mizokawa, Z. X. Shen, A. Fujimori, T. Kakeshita, H. Eisaki and S. Uchida, *Phys. Rev. B* **62**, 4137 (2000).
- [17] E. Razzoli, G. Drachuck, A. Keren, M. Radovic, N. C. Plumb, J. Chang, Y. B. Huang, H. Ding, J. Mesot and M. Shi, *Phys. Rev. Lett.* **110**, 047004 (2013).
- [18] Y. Peng, J. Meng, D. Mou, J. He, L. Zhao, Y. Wu, G. Liu, X. Dong, S. He, J. Zhang, *Nature Communications* **4**, 2459 (2013).
- [19] K. M. Shen, T. Yoshida, D. H. Lu, F. Ronning, N. P. Armitage, W. S. Lee, X. J. Zhou, A. Damascelli, D. L. Feng, N. J. C. Ingle, H. Eisaki, Y. Kohsaka, H. Takagi, T. Kakeshita, S. Uchida, P. K. Mang, M. Greven, Y. Onose, Y. Taguchi, Y. Tokura, S. Komiya, Y. Ando, M. Azuma, M. Takano, A. Fujimori, Z. X. Shen, *Phys. Rev. B* **69**, 054503 (2004).
- [20] G. E. Volovik, *JETP Lett.*, **66**, 527 (1997).
- [21] R. B. Laughlin, *Phys. Rev. Lett.* **80**, 5188 (1998).
- [22] T. Senthil, J. B. Marston and Matthew P. A. Fisher, *Phys. Rev. B* **60**, 4245 (1999).
- [23] A. Altland and M. R. Zirnbauer, *Phys. Rev. B* **55**, 1142 (1997).
- [24] A. P. Schnyder, S. Ryu, A. Furusaki and A. W. W. Ludwig, *Phys. Rev. B* **78**, 195125 (2008).
- [25] Xiao-Liang Qi, Taylor L. Hughes and S. C. Zhang, *Phys. Rev. B* **82**, 184516 (2010).
- [26] A. A. Zyuzin and A. A. Burkov, *Phys. Rev. B* **83**, 195413 (2011).
- [27] A. Cook and M. Franz, *Phys. Rev. B* **84**, 201105(R) (2011).
- [28] B. Lake, H. M. Rønnow, N. B. Christensen, G. Aeppli, K. Leffmann, D. F. McMorrow, P. Vorderwisch, P. Smeibidl, M. Mongkorntong, T. Sasagawa, M. Nohara, H. Takagi, and T. E. Mason, *Nature (London)* **415**, 299 (2002).
- [29] Yuan-Ming Lu, Tao Xiang and Dung-Hai Lee, arXiv.1311.5892 v1 [cond-mat.supr-con] 22 Nov. (2013).